Available online at www.sciencedirect.com

Journal of Acupuncture and Meridian Studies

journal homepage: www.jams-kpi.com

RESEARCH ARTICLE

Development and Evaluation of a Multi-frequency Bioelectrical Impedance Analysis Analyzer for Estimating Acupoint Composition

Soo-Byeong Kim [1], Na-Ra Lee [1], Tae-Min Shin [2], Yong-Heum Lee [1,*]

[1] *Eastern & Western Biomedical System Lab, Department of Biomedical Engineering, Yonsei University, Wonju, Gangwon-Do, South Korea*
[2] *Medical Computer System Lab, Department of Biomedical Engineering, Yonsei University, Wonju, Gangwon-Do, South Korea*

Available online 21 February 2013

Received: Aug 30, 2012
Revised: Jan 19, 2013
Accepted: Jan 22, 2013

KEYWORDS
acupoint;
acupoint potential;
bio-ion;
bioelectrical impedance analysis (BIA)

Abstract
The purpose of this study was to suggest a new method of estimating acupoint compositions by using a multi-frequency bioelectrical impedance analysis (MF-BIA) method at 5 kHz, 50 kHz and 200 kHz within 2 cm of acupoints divided into local segments. To verify the system developed, we confirmed the stable occurrence of a constant current at every frequency, regardless of the impedance connected to the electrodes. Moreover, we found left and right distal bicep brachii aponeurosis to be identical by using ultrasound imaging, and we analyzed the repeatability of the findings by making 10 consecutive sets of measurements ($p > 0.05$). To evaluate the practical use of the acupoint composition, we used the MF-BIA analyzer to measure the left and right LU3, LU4, and LU9 at the lung meridian. We confirmed that the potentials generated were equal to the changes in the cell membrane function, which were caused by the applied frequency ($p < 0.01$). We also verified that the MF-BIA analyzer measurements corresponded to the acupoint components by comparing the left and right potentials generated ($p > 0.05$). Hence, we conclude that the MF-BIA analyzer can be used to estimate the acupoint composition based on the acupoint state.

* Corresponding author. Laboratory of Eastern & Western Biomedical System, Department of Biomedical Engineering, Yonsei University, 1 Yonseidae-gil, Wonju, Gangwon-do, South Korea.
E-mail: koaim@yonsei.ac.kr (Y.-H. Lee).

pISSN 2005-2901 eISSN 2093-8152
http://dx.doi.org/10.1016/j.jams.2013.01.021

1. Introduction

Regardless of whether it takes place in the East or the West, the discussion of the importance of body composition assessment is invigorated in various research areas, such as nutritional science and sports medicine. To evaluate body composition, various methods such as magnetic resonance imaging, computed tomography and isotope dilution analysis have been suggested. However, these methods have limitations for practical use for spatial and financial reasons, and they also require skilled professionals [1].

Bioelectrical impedance analysis (BIA) has been proposed to overcome these issues because it measures body composition quickly and conveniently in a non-invasive manner [2,3]. BIA obtains impedance measurements of body composition by penetrating a small alternating current of 800 μA through the human body [4]. Cells in the tissues are composed of extracellular fluid, intracellular fluid and the cell membrane. The cell membrane electrically acts as a capacitor. Most electrolytes are found in the intracellular and extracellular fluid due to the insulating properties of the cell membrane. Cells have different electrical properties that are influenced by both the cell membrane and the gradient of electrolytes between the intracellular and the extracellular fluid. Therefore, all cells in muscular and osseous tissues have their own unique electric properties. A wide frequency band from 1 kHz to 1 MHz is used in BIA to identify the frequencies that reflect various conditions of electrolytes at the cellular level. As a result, a current with a frequency of around 50 kHz can penetrate the cell membrane, and currents with lower frequency bands from 1 kHz to 20 kHz pass through to the extracellular fluid. Moreover, it has been reported that a current with a frequency band from 100 to 200 kHz passes through both the extracellular and intracellular fluid by the loss of the cell membrane [5–7]. According to this previous study, BIA is universally used as follows: 5 kHz to estimate the extracellular fluid; 50 kHz to determine the distinction of skeletal muscle characteristics; and 200 kHz to identify the total amount of intracellular and extracellular fluid.

The BIA technique has been suggested as a useful tool to analyze body composition based upon the close, direct relationship between impedance data and total body water [8,9]. BIA is a total body water estimation tool that is based upon the role of electrolytes as conductors. The impedance of adipose tissue is relatively high due to the limitation of body fluid in that type of tissue. In contrast, it is reported that fat-free mass, which includes everything that is not body fat, has a relatively lower impedance. Therefore, BIA is used as a method to assess both the fat-free mass and the degree of obesity in the entire body or one particular segment of it [10,11].

In Korean medicine, most diagnosis and treatment procedures are based upon the meridian theory that argues that acupoints and internal organs are connected by meridians, which are pathways for life energy (Qi). In other words, 12 meridians represent the human body's overall physical and pathological conditions, which appear externally through acupoints. An acupoint is regarded as a stimulating point for treatment and a reaction point for diagnosis. However, it is difficult to measure and analyze the state of an acupoint for its meridian and its conditions. Thus, it is necessary to propose and develop a new meridian diagnostic method.

This study suggests a new diagnostic method that applies a multi-frequency BIA analyzer at an acupoint. A reinterpretation will be possible from the perspective of Korean medicine through the detection of the amount of both intracellular and extracellular fluids at acupoints. For this purpose, the six-channel multi-frequency BIA (MF-BIA) analyzer was developed to generate 5 kHz, 50 kHz and 200 kHz frequencies with 800 μA current.

The generated potential was measured from 100 Ω to 600 Ω to confirm that the current was constant at 800 μA, irrespective of the impedance connected to the electrodes of the MF-BIA analyzer. It was an attempt to assess the generated potential accuracy of pure resistance through a comparative analysis between the generated potential and the calculated prediction value. Every segment of the human body consists of unique muscular and osseous tissues. Therefore, each section of the human body has unique cell membrane properties, such as how well it insulates and the different distributions of electrolytes in the intracellular and extracellular fluids. As a result, the capacitance of the cell membrane is different in every segment of the human body, and its conductance ability is influenced by the amount of electrolytes each section contains.

When applied to the same segment of the human body on an identical participant, the generated potential measurement, which is influenced by the same cell membrane and electrolytes in the intracellular and extracellular fluids, must have high repeatability. It is therefore necessary to ensure the accuracy and repeatability of the generated potential measurements; those taken from corresponding left and right locations in the same participant should have no significant differences because the human body has an identical anatomical structure on the left and the right sides. We found identical anatomical areas of the left and right biceps brachii using the ultrasound images and tested the repeatability of the local segment's generated potential for each frequency. To confirm the practical use of the MF-BIA analyzer's acupoint composition measurement functions, the left and the right LU3, LU4, and LU9 at the lung meridian (LU) were analyzed.

This study suggested a new meridian diagnostic method by obtaining sufficient data that can be put to practical use in Korean medicine based upon our accuracy evaluation of the system.

2. Materials and methods

2.1. Principles of the MF-BIA analyzer

Fig. 1 is an equivalent circuit diagram that illustrates the electric current flow when an 800-μA current was applied to a cell or a tissue. C_m and R_m signify the capacitance and the resistance of each cell membrane, respectively, and R_i and R_e show the resistance of the intracellular and extracellular fluid, respectively. Each of the continuous lines and the dotted lines represent the electric current flow of

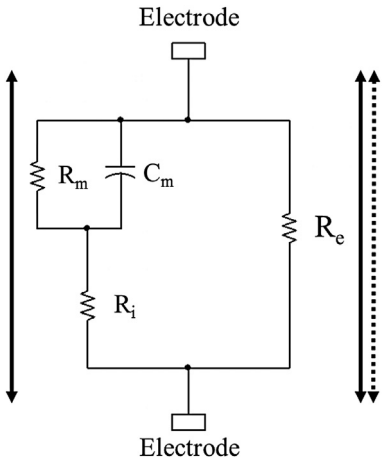

Figure 1 Equivalent circuit for impedance in a cell or tissue. C_m: membrane capacitance, R_m: membrane resistance, R_e: extracellular fluid resistance, R_i: intracellular fluid resistance, continuous line: current flow of high frequency, dotted line: current flow of low frequency.

the high and low frequencies, respectively. The electric current of the low frequency signal flows mostly into the extracellular fluid and is affected by the resistance of R_e. The high frequency enables the loss of the cell membrane function as an insulator, and the impedance is lowered to $R_iR_e/(R_i+R_e)$. As a result, the current passes completely through the intracellular fluid. In the MF-BIA analyzer, bioelectrical impedance changes depend on the frequency of the signal. Hence, the MF-BIA analyzer provides a method by which to measure the potential generated by these changes [12,13].

2.2. Development of the MF-BIA analyzer to estimate the acupoint composition

In this study, three frequencies (5 kHz, 50 kHz and 200 kHz) were chosen to estimate the amount of intracellular and extracellular fluid. The system was designed to generate an 800-μA constant current at each of the three frequencies. The noise components of the generated potential were removed by a 482-Hz, second-order high-pass filter and a 530-kHz, second-order low-pass filter. Then, the signal was amplified by 8.2 gain and converted to a digital signal in the form of 10 bits by 100 samples in 1 second (Fig. 2).

Since each measurement of impedance in the tissues has a slightly different capacitance and resistance, the segments of the human body that include acupoints are not considered to have a cylindrical shape of a uniform, cross-sectional area. Hence, when there is a difference of 1 cm in the interval between electrodes, the error of the measured electrode ranges from 2% to 16% and is usually a result of the influence of another tissue [14]. Dry electrodes are suitable to use in long-term monitoring, and it is easy to design them to be sufficiently small to detect close intervals and local points. Dry electrodes are widely used to avoid the adhesives or gel membranes required with wet electrodes. Considering the interval between acupoints and the small size of an acupoint, it was proper to use dry electrodes and manual acupuncture needles in this study. However, dry electrodes can be influenced by the interference of noise, such as motion artifacts and power line. Moreover, dry electrodes are susceptible to the interference of noise due to the high contact impedance between the skin and the electrode. As a result, dry electrodes generate measurement errors due to the mismatch between electrodes, which can cause common-mode voltage and saturate the signal [15]. We therefore used wet

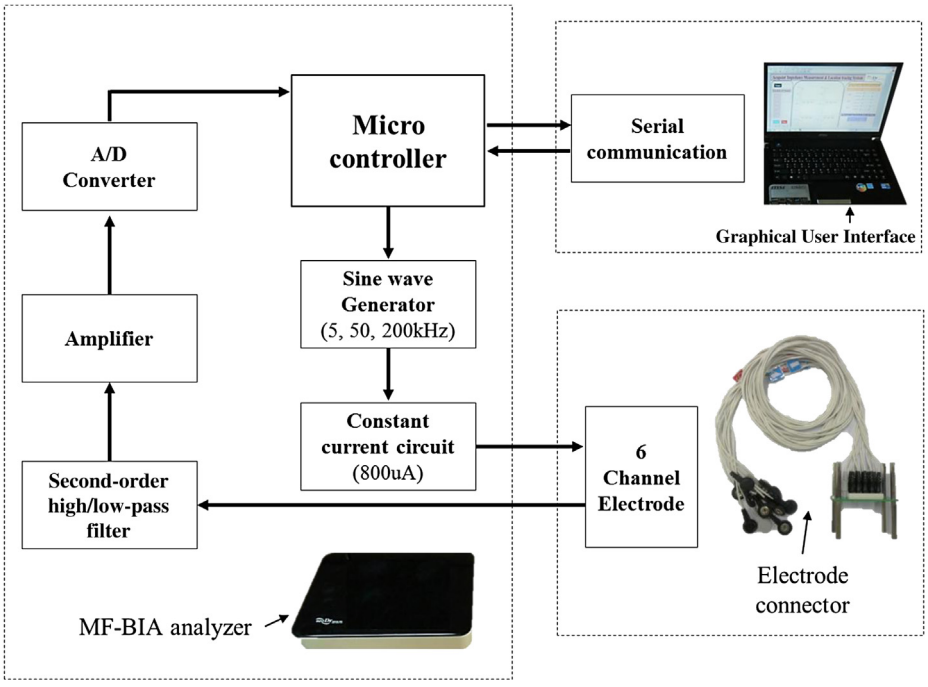

Figure 2 Block diagram of the MF-BIA analyzer.

electrodes, which are available and can maintain a small interval and size taking into consideration the priorities on identification of practical use rather than the interval between acupoints and the small size of an acupoint. To reduce the operator experimental error and signal noise, two circular silver/silver chloride (Ag/AgCl) surface electrodes (Noraxon Inc., US) that maintained a constant distance were chosen. These electrodes had 18 mm of constant distance between them and are subminiature Ag/AgCl electrodes with a diameter of 14 mm (Fig. 3). By using a topical skin adhesive electrode, we tried to maintain a constant pressure and reduce the errors that can arise from tiny motions.

2.3. Evaluation of the MF-BIA analyzer

The generated potential was measured from 100 Ω to 600 Ω by increasing the potential by 50 Ω after every 10 sets. Using the SONOACE X8 (Samsung Medison Inc., Korea) ultrasound imaging system, we found the left and right distal biceps brachii aponeurosis and then measured 10 consecutive sets of the generated potentials.

2.4. Evaluation method to identify the usefulness of the MF-BIA analyzer to estimate acupoint composition

To confirm the practical use of the generated potential of the MF-BIA analyzer, the left and right LU3, LU4 and LU9 acupoints were selected. Each acupoint was measured in three sets with 1-minute intervals at 5 kHz, 50 kHz and 200 kHz. The acupoints at LU3 and LU4 had similar body compositions because they are closely located in the biceps brachii. Therefore, these two acupoints were selected to confirm the application and availability of the acupoint characteristics located in identical contralateral musculoskeletal structures. In addition, LU9, which is located on the radial artery between the radial styloid process and the scaphoid bone, was selected because of the different body composition due to the different musculoskeletal structure (Fig. 4).

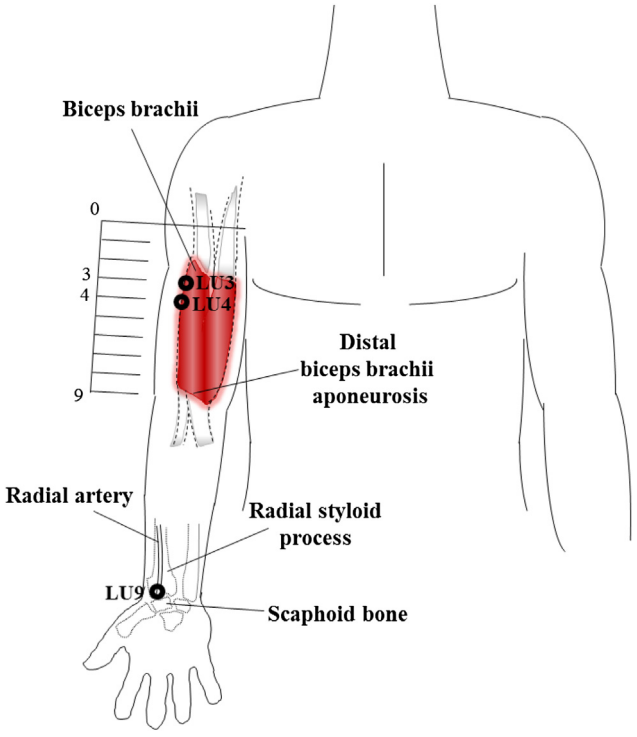

Figure 4 The locations of acupoints LU3, LU4 and LU9.

2.5. Participants

All study participants were adult males who had not received treatment for any diseases in the previous year and who had no difficulties performing their daily activities. For the MF-BIA analyzer performance evaluation, 10 people (age: 23 ± 2 years, height: 175.75 ± 5.38 cm, body mass: 73.25 ± 18.14 kg) were studied. To detect the generated potential, 11 adult men (age: 27 ± 2 years, height: 175.8 ± 5.23 cm, body mass: 75.6 ± 18.70 kg) voluntarily participated, and all participants were limited to persons who had no burns or other injuries on their skin near the acupoints. Additionally, those who had participated in the MF-BIA analyzer performance evaluation were excluded.

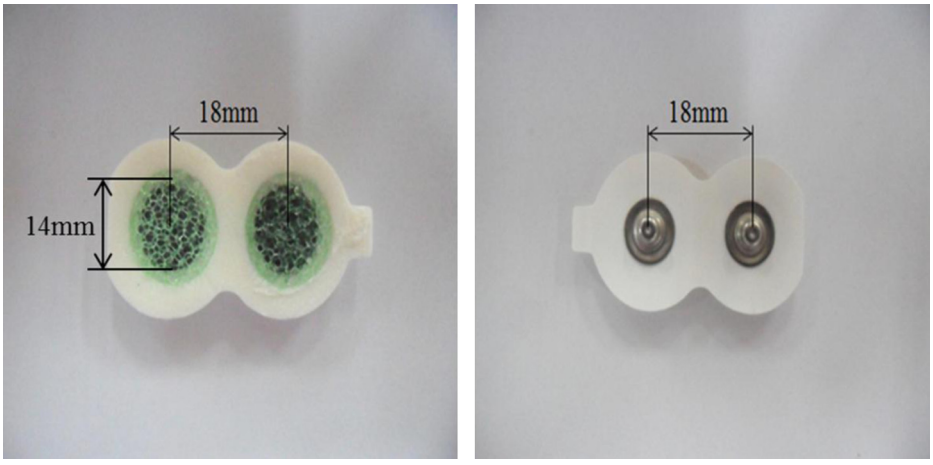

Figure 3 Electrodes for the bioelectrical impedance measurement, which were chosen to minimize the experimental errors caused by adhesive electrodes.

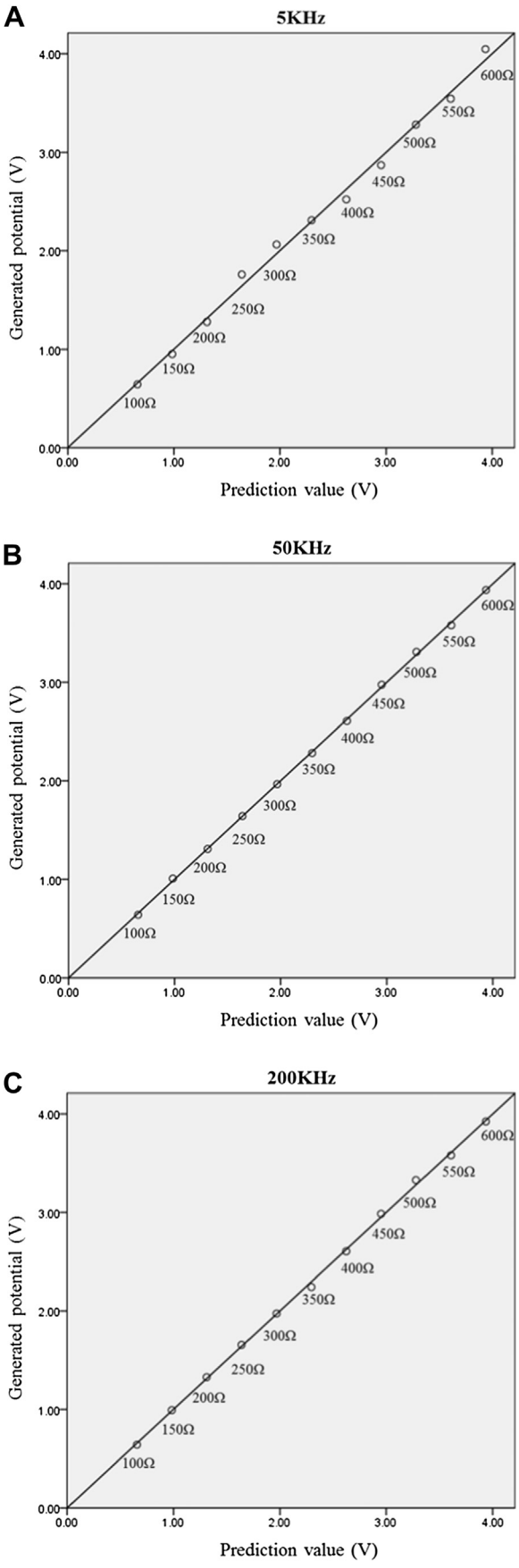

Following the general BIA measurement standard, all participants maintained 45 degrees of abduction of both the upper and lower limbs to prevent each segment being in contact. The positions in both femoral regions were also maintained without contact. Before attaching the electrodes, all acupoints were medically sterilized.

When the experimental environment temperature is below 14°C, it causes a significant increase in the human body resistance by reducing the skin temperature [16]. Hence, the clinical laboratory temperature was maintained at 25°C to prevent drops in the temperature of the skin. The main cause of errors arising from the participants' conditions was a change in hydration status, which is typically precipitated by eating a meal, fluid intake, dehydration and exercise, and can alter bioelectrical impedance. After eating, approximately 13–17 Ω of the resistance decreases within 2–4 hours [17]. Moreover, after drinking 1 L of fluid, the resistance is increased by approximately 10 Ω after 4 minutes [16]. The following conditions proposed by previous researchers were taken into consideration and were limited in the participants:

- urination within the previous 30 minutes;
- fluid or food intake within the last 4 hours;
- exercise within the past 12 hours;
- alcohol intake within the previous 48 hours; and
- diuretic administration in the past 7 days.

2.6. Statistics

A simple linear regression was used for constant current occurrence confirmation during the system assessment. Also, the contrast test was based on a one-way repeated measures analysis of variance (ANOVA) and was used to assess the degree of repeatability. To confirm any significant differences between the left and right distal biceps brachii aponeurosis, the generated potential was modified in the form of normalization based on the left- side generated potential, and an independent *t*-test was conducted. A one-way ANOVA was used to compare the differences according to the frequencies caused by each acupoint. An independent t-test was conducted to examine the significant differences between the matching left and right acupoints. Additionally, to analyze the differences between each acupoint, least significant difference (LSD) analysis was used in the one-way ANOVA's *post-hoc* comparison. For the specificity analysis, the generated potential at each right-sided acupoint was normalized with the generated potential at each left-sided acupoint to confirm any significant differences between the corresponding acupoints on the left and right. The generated potentials at the left acupoints were divided by our own value, considered to be 1. The generated potentials in the right acupoints were divided by the generated potentials of the corresponding left acupoints. The significance level of the statistical analysis was set at $p < 0.05$.

Figure 5 Results of the 800 μA constant current generation evaluation. (A) Results of a simple linear regression at 5 kHz ($R^2 = 0.995$); (B) results of a simple linear regression at 50 kHz ($R^2 = 0.999$); and (C) results of a simple linear regression at 200 kHz ($R^2 = 0.999$).

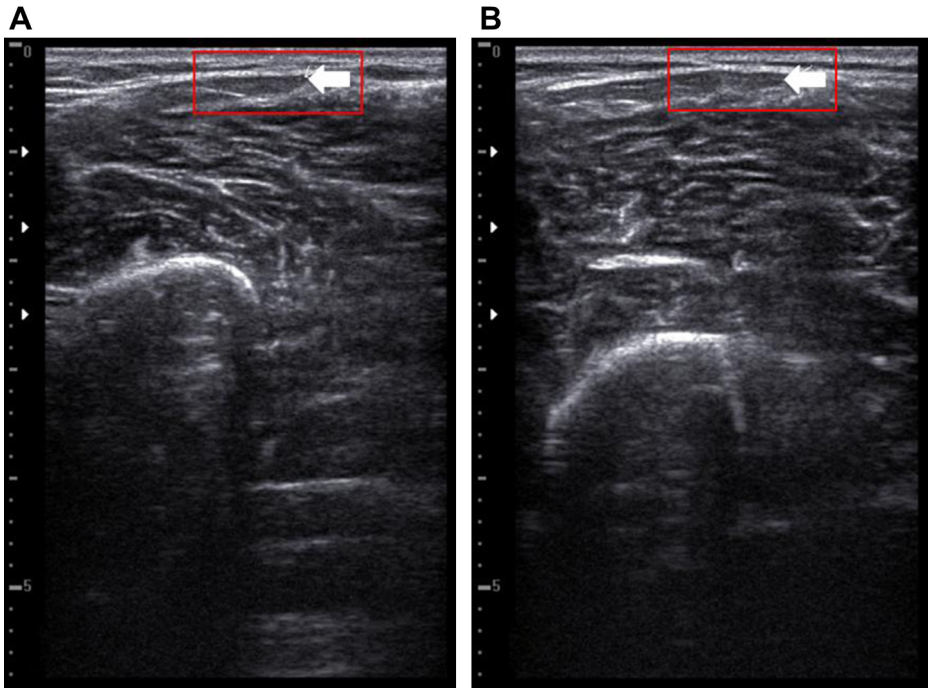

Figure 6 Ultrasound images of the left and right distal biceps brachii aponeurosis. (A) Left distal biceps brachii aponeurosis (arrow); and (B) right distal biceps brachii aponeurosis (arrow).

3. Results

3.1. Results of the 800 μA constant current generation evaluation of the MF-BIA analyzer

We observed that the increase in the generated potential was proportional to the increase in the resistance. A simple linear regression that analyzed the generated potential and the calculated prediction value confirmed a high linearity of 0.995, 0.999 and 0.999 in each R-square of 5 kHz, 50 kHz and 200 kHz, respectively (Fig. 5).

3.2. Results of the measurement repeatability evaluation of the MF-BIA analyzer

Fig. 6 shows the ultrasound images of the left and right distal biceps brachii aponeurosis. Table 1 displays the results of the contrast test based on the one-way repeated measures ANOVA. The results of each significant difference between the rest of the generated potentials and the first generated potential, which is regarded as a reference in every participant, are also shown in Table 1. Significant differences in the repeatedly generated potentials in both the left and right distal biceps brachii aponeurosis were not found at all frequencies ($p > 0.05$). Table 2 shows the results of the independent *t*-test that analyzed the significant differences between the left and right distal biceps brachii aponeurosis. The results of the independent *t*-test indicated that differences between the left and right distal biceps brachii aponeurosis were not observed for every frequency ($p > 0.05$).

3.3. Results of the usefulness evaluation of the MF-BIA analyzer in estimating acupoint composition

Analysis of the generated potential measurements of the identical acupoints on the left and right sides.

Fig. 7 shows the generated potentials of the identical acupoints in the left and right in order of frequency. After conducting the one-way ANOVA at every frequency, we confirmed that all acupoints had a significant difference at each frequency ($p < 0.01$). It was also observed that the generated potential was the highest at 5 kHz, and the lowest was seen at 200 kHz. Table 3 displays the independent *t*-test results of the left and right generated potentials. As a result, there was no significant difference in the corresponding acupoints ($p > 0.05$).

Table 1 Significant probability analysis results of measurement repeatability: the results of a contrast test based on a one-way repeated measures analysis of variance. The main criteria were the first measurements.

Measurement	5 kHz	50 kHz	200 kHz
	p	*p*	*p*
2nd	0.860	0.317	0.599
3rd	0.587	0.803	0.941
4th	0.139	0.455	0.319
5th	0.911	0.125	0.584
6th	0.447	0.272	0.737
7th	0.190	0.387	0.724
8th	0.234	0.122	0.064
9th	0.494	0.107	0.053
10th	0.226	0.648	0.229

Table 2 Independent *t*-test results of the left and right distal biceps brachii aponeurosis ($n = 10$).

	5 kHz	50 kHz	200 kHz
p	0.099	0.994	0.112

Analysis of the significant differences between acupoints.

The results of the generated potential of all acupoints at each frequency are shown in Fig. 8. Table 4 shows the results of a *post-hoc* LSD analysis of the one-way ANOVA. As a result, no significant differences were observed between LU3 and LU4 at any frequency ($p > 0.05$), but significant differences at all frequencies between LU9 and LU3 or LU4 were confirmed ($p < 0.05$).

Analysis of the specificity in two participants.

In nine out of 11 participants there were no significant differences between identical corresponding acupoints on the left and right sides. In the remaining two cases, there were significant differences in the generated potentials between the contralateral acupoints on the left and right.

Fig. 9 displays the results of the normalized generated potential at LU3 of these two participants. In both males, the highest difference was observed at 5 kHz. Significant differences at 5 kHz were confirmed as 67.91 ± 2.29% in participant 1 and 109.17 ± 10.20% in participant 2. At 50 kHz, a significant difference was observed at 78.14 ± 0.8% in participant 1, but there was no significant difference found with 104.32 ± 6.21% in participant 2. Finally, at 200 kHz, the lowest differences were observed with 83.51 ± 9.14% in participant 1 and at 99.37 ± 10.28% in participant 2.

Fig. 10 is the result of the normalized generated potential at LU4 for the two participants. The highest difference in participant 1 was observed at 5 kHz, with 43.63 ± 2.69 %. In participant 2, the highest difference was found at 200 kHz with 31.34 ± 0.42%. The highest differences were over 60%. Moreover, significant differences in participant 1 were also seen at 50 kHz with 74.63 ± 7.69% and at 200 kHz with 76.61 ± 7.86%. In participant 2, there were no significant differences at 5 kHz, with 102.33 ± 2.52%, and at 50 kHz, with 101.64 ± 1.31%.

Fig. 11 is the result of the normalized generated potential at LU9 for the two participants. In participant 1, significant differences were observed with 77.98 ± 1.83%, 83.61 ± 0.19% and 89.85 ± 1.31% in order of frequency. In participant 2, there were no significant differences at 5 kHz with 102.66 ± 3.39%, at 50 kHz 107.02 ± 0.63% or at 200 kHz with 109.09 ± 0.00%.

4. Discussion

The current is a fixed value therefore the generated potential can only be influenced by the resistance. We observed that the generated potentials were equal to the prediction values with a high linearity in every frequency. Hence, we confirmed the stable occurrence of a constant current for every frequency. We also observed that the generated potentials at each frequency were proportional to the resistance and confirmed the presence of a constant current of 800 μA regardless of the impedance connected to the electrodes. Furthermore, to identify the strong accuracy and repeatability of the generated potentials at

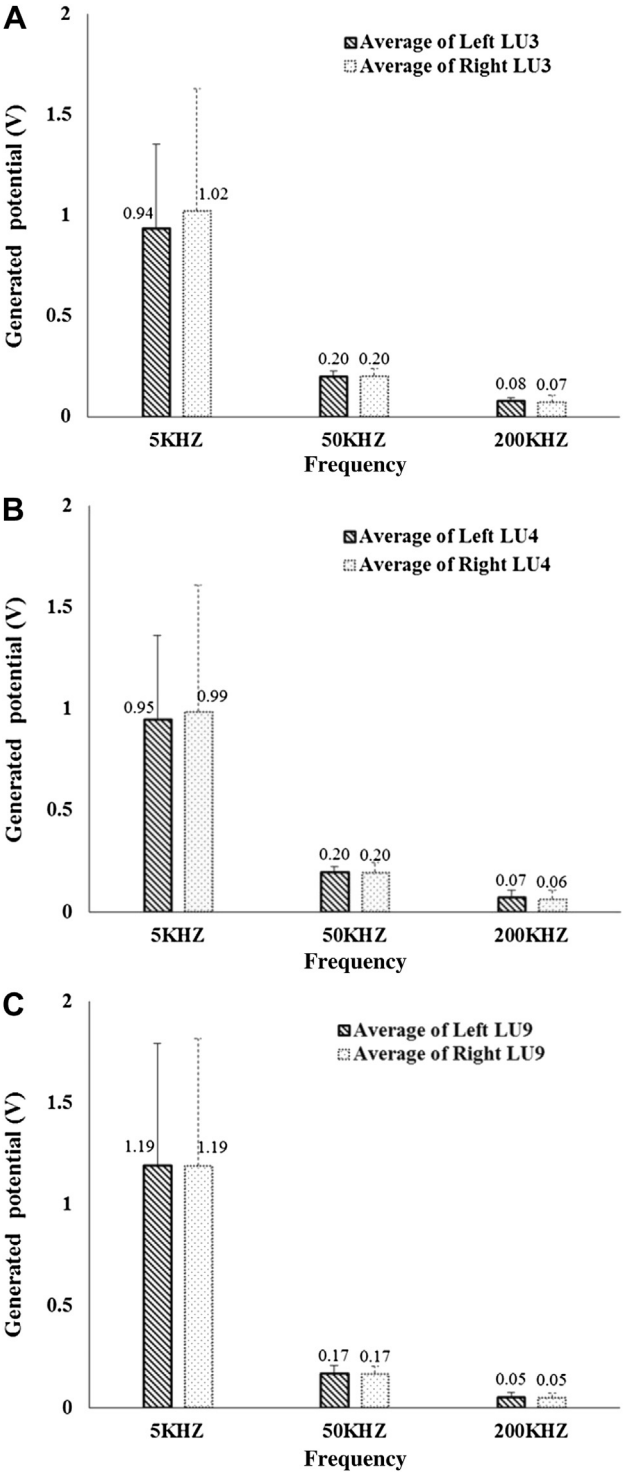

Figure 7 Analysis of the generated potential of identical acupoints on the left and right sides ($n = 11$). (A) Analysis of the generated potential of the left and right LU3; (B) analysis of the generated potential of the left and right LU4; and (C) analysis of the generated potential of the left and right LU9.

Table 3 Independent t-test results of the identical acupoints on the left and right sides ($n = 11$).

Frequency	p		
	LU3	LU4	LU9
5 kHz	0.531	0.788	0.990
50 kHz	0.860	0.828	0.890
200 kHz	0.330	0.348	0.409

contralateral anatomical positions, an ultrasound imaging system was used to find the left and right distal biceps brachii aponeurosis. There were no significant differences between repeatedly measured data in each frequency ($p > 0.05$). As a result, we confirmed that the repeated generated potential was affected by the capacitive resistance of the cell membrane, and the resistance caused by the electrolytes in the intracellular and extracellular fluids had no significant differences at identical positions on opposite sides of the body. Moreover, the independent *t*-test results for every frequency between the left and right distal biceps brachii aponeurosis indicated that there were no significant differences in the anatomical structure of the two sides. In anatomically identical positions on the left and right, the extracellular and intracellular fluids' structural components were very similarly distributed. Therefore, we concluded that the strong correlation between the left and right positions was reflected by each similar capacitive reactance by the cell membranes and the similar resistance by the electrolytes in the intracellular and extracellular fluids on the left and right.

The generated potentials of the left and right LU3, LU4, and LU9 were analyzed to confirm the practical use of the MF-BIA analyzer. The results indicated that the generated potential was the highest at 5 kHz and the lowest at 200 kHz ($p < 0.01$). These findings are identical to the results of a previous study, which reported decreases in impedance due to the loss of cell membrane function at high frequencies [5–7]. No significant differences were observed between LU3 and LU4 ($p > 0.05$) at any frequency. However, significant differences were confirmed between LU3, LU4, and LU9 ($p < 0.001$). We speculated that LU3 and LU4 did not show significant differences because both exist on the biceps brachii. The LU9 is situated between the radial styloid process and the scaphoid bone. Therefore, LU9 contains different muscular and osseous tissue than LU3 and LU4. Significant differences were likely observed between LU3, LU4, and LU9 due to their different anatomical positions.

To analyze any significant differences in the generated potentials of the left and right identical acupoints in every participant, we normalized the generated potential of the right acupoint based on the generated potential of the left acupoint and then analyzed the difference. In most participants, there were no significant differences in the generated potentials of the corresponding left and right acupoints for each frequency. These findings suggest that left- and right-sided acupoints were positioned in an anatomically equivalent area and also that the participants had similar body compositions. Furthermore, discrepancies of the left and right generated potentials were observed in

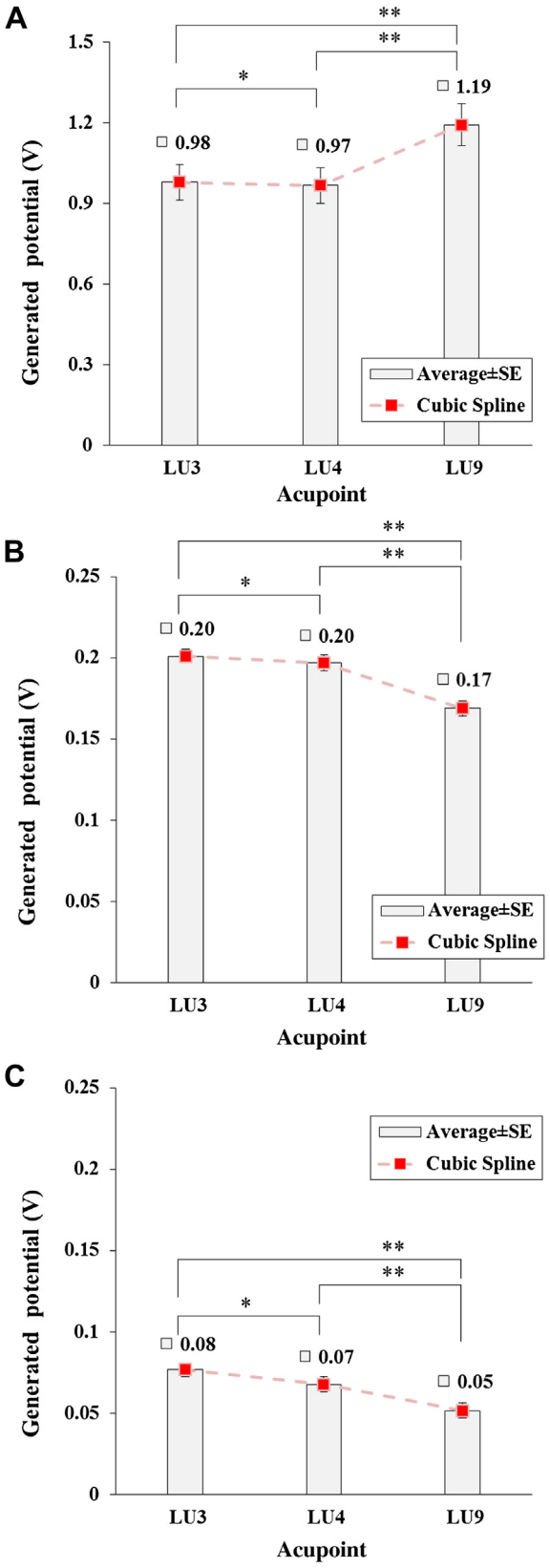

Figure 8 Analysis of the differences in the generated potential according to the acupoint's position ($n = 11$): (A) 5 kHz; (B) 50 kHz; and (C) 200 kHz. (*$p > 0.05$ and **$p < 0.05$).

Table 4 Analysis of the differences in the generated potentials according to the acupoint's position by *post-hoc* least significant difference (LSD)-analysis.

		p		
		LU3	LU4	LU9
LU3	5 kHz	—	0.909	0.035
	50 kHz	—	0.514	<0.001
	200 kHz	—	0.108	<0.001
LU4	5 kHz	0.909	—	0.026
	50 kHz	0.514	—	<0.001
	200 kHz	0.108	—	0.004
LU9	5 kHz	0.035	0.026	—
	50 kHz	<0.001	<0.001	—
	200 kHz	<0.001	0.004	—

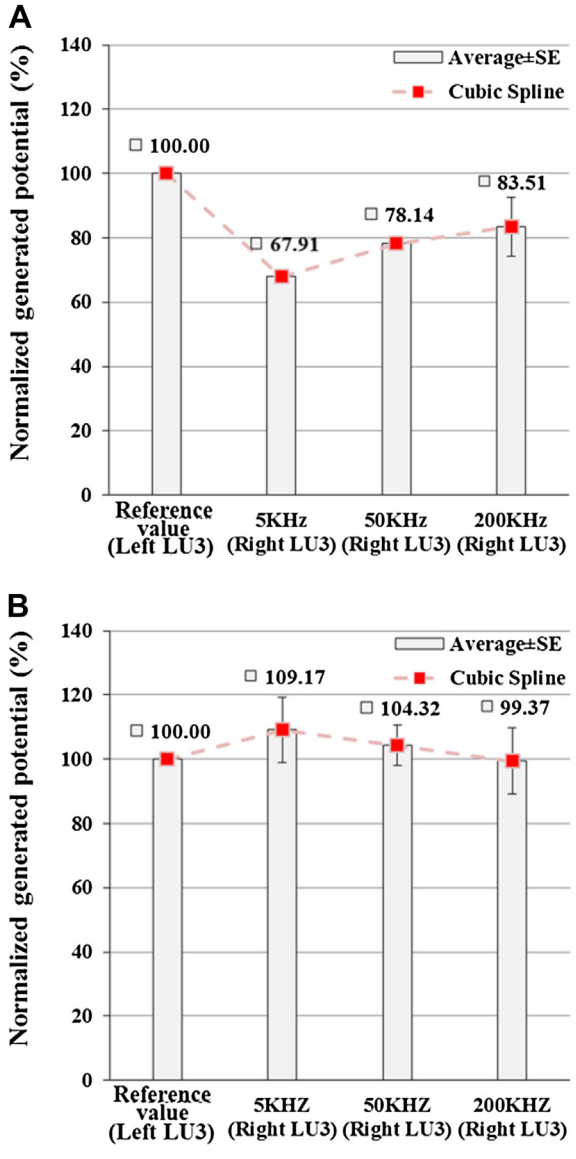

Figure 9 Analysis of the differences in the generated potentials of the left and right sides at LU3. The reference value is the normalization value of the left LU3 normalized by the measured value at 5 kHz, 50 kHz, and 200 kHz. (A) Participant 1; and (B) Participant 2.

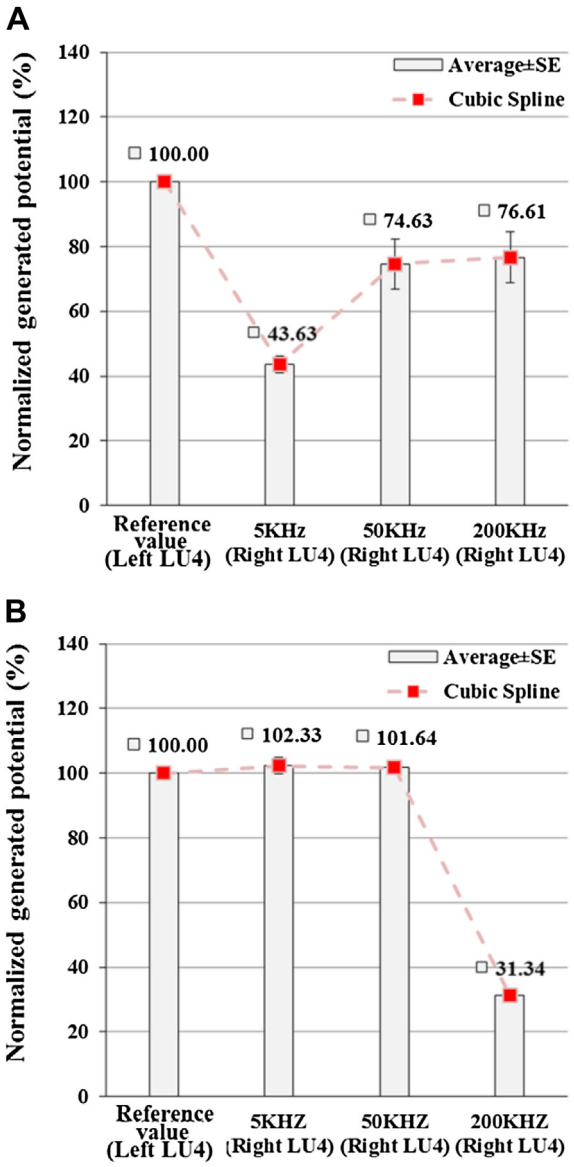

Figure 10 Analysis of the differences in the generated potentials of the left and right sides at LU4. The reference value is the normalization value of the left LU4 normalized by the measured value at 5 kHz, 50 kHz and 200 kHz. (A) Participant 1, and (B) Participant 2.

two participants. At 5 kHz, significant differences between the left and right sides were noted at all acupoints of participant 1 and at LU3 of participant 2.

BIA has long been used as a simple and noninvasive technique to assess limb composition [18—20]. Validation between anthropometry and BIA at appendicular tissues has been conducted against computed tomography, magnetic resonance imaging and dual-energy X-ray absorptiometry. Previous results have shown that BIA is a technique that produces highly accurate estimates of appendicular tissues in healthy participants [21—23]. Hence, a strong correlation between corresponding left and right acupoints is considered a reflection of the capacitive reactance of the cell

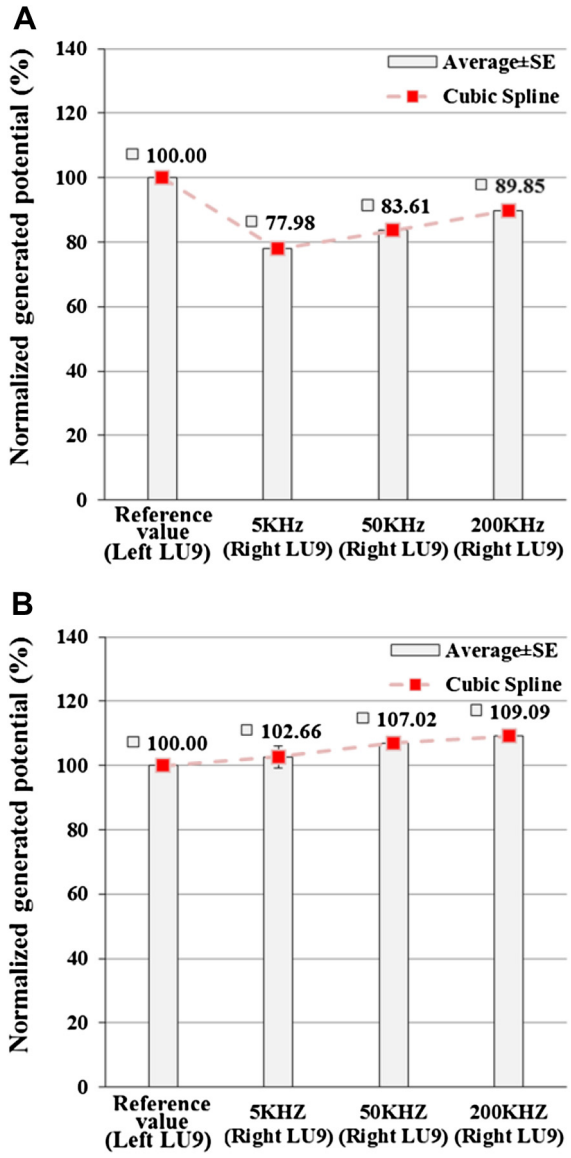

Figure 11 Analysis of the differences in the generated potentials of the left and right sides at LU9. The reference value is the normalization value of the left LU9 normalized by the measured value at 5 kHz, 50 kHz and 200 kHz. (A) Participant 1, and (B) Participant 2.

membranes and resistance by the electrolytes in the intracellular and extracellular fluids.

Exercise-induced ion shifts, physicochemical reactions and metabolic processes lead to ion concentration changes in compartments proximal to the sarcolemma. Multiple ionic compartment changes [K^+, Na^+, Ca^{2+}, Cl^-, H^+, HCO_3^-, Mg^{2+}, $H_2PO_4^-$, PCr^{2-}, lactate$^-$] have been observed with intense exercise or electrical stimulation [24]. According to previous research, an elevated K^+ gradient in the extracellular fluid can reduce the maximal muscle force and enhance local blood flow [25,26]. Furthermore, a lowered Na^+ gradient in the extracellular fluid acts synergistically with the raised K^+ gradient [27,28]. The H^+ gradient in both the intracellular and extracellular fluids increases to restore the raised K^+ gradient in the extracellular fluid [29,30]. In amphibian muscle, the Ca^{2+} gradient in the intracellular fluid is lowered to allow for impaired excitability during fatigue [31,32]. Because of these responses, we considered the cases with differences in the left- and right-generated potentials to be indicative of an imbalance in the intracellular and extracellular fluids based on the participant's condition in every frequency. In the case of LU4 in participant 2, no significant differences existed at 5 kHz and 50 kHz but were observed at 200 kHz. This result was considered to be the lowest ionic compartment gradient in the intracellular fluid.

5. Conclusions

In this study, a six-channel MF-BIA analyzer, which measures and assesses the structural components of the local positions of acupoints, was developed to observe the electric uniqueness of the components in the acupoint structure using MF-BIA. Our study confirmed that an 800-μA constant current occurred regardless of the impedance connected to the MF-BIA analyzer and identified the estimation accuracy of pure resistance. Additionally, the measurements and the correspondence of the generated potentials of the left and right equivalent positions were repeatable by applying the MF-BIA analyzer to local segments of the body. To verify the practical use of the MF-BIA analyzer in the structural component distinction of acupoints, generated potential measurements were taken, compared and analyzed from LU3, LU4, and LU9. The results showed that the generated potentials were equal to the changes of the cell membrane function, which were caused by the applied frequencies. By comparing the generated potential measurements of the left and right acupoints obtained with the MF-BIA analyzer, we confirmed correspondence with the acupoint components. Furthermore, the feasibility of estimating the generated potential specificity at acupoints was checked using two participants in the study. The study concluded that the MF-BIA analyzer was able to estimate acupoint composition based on the acupoint state, and we propose it as a new evaluation method of meridians and acupoints.

Disclosure statement

The author affirms there are no conflicts of interest and the author has no financial interest related to the material of this manuscript.

Acknowledgments

This work was supported by the Technology Innovation Development Program (SA113768) of the Small and Medium Business Administration, Korea.

References

1. Panotopoulos G, Ruiz JC, Guy-Grand B, Basdevant A. Dual x-ray absorptiometry, bioelectrical impedance, and near infrared

interactance in obese women. *Med Sci Sports Exerc*. 2001;33: 665—670.
2. Hoffer BC, Meador CK, Simpson DC. A relationship between whole body impedance and total body water volume. *Ann N Y Acad Sci*. 1970;170:452—461.
3. Nyboer J. Percent body fat by four terminal bio-electrical impedance and body density in college freshmen. In: *Proceedings of the 5th International Conference on Electrical Bio-Impedance*. Tokyo: Japan; August, 1981.
4. Kyle UG, Bosaeus I, De Lorenzo AD, Deurenberg P, Elia M, Gómez JM, et al. Bioelectrical impedance analysis—part I: review of principles and methods. *Clin Nutr*. 2004;23:1226—1243.
5. Miyatani M, Kanehisa H, Fukunaga T. Validity of bioelectrical impedance and ultrasonographic methods for estimating the muscle volume of the upper arm. *Eur J Appl Physiol*. 2000;82: 391—396.
6. Miyatani M, Kanehisa H, Masuo Y, Ito M, Fukunaga T. Validity of estimating limb muscle volume by bioelectrical impedance. *J Appl Physiol*. 2001;91:386—394.
7. Nakadomo F, Tanaka K, Hazama T, Maeda K. Assessment of body composition by bioelectrical impedance analysis: effects of skin resistance on impedance. *Ann Physiol Anthropol*. 1990; 9:109—114 [In Japanese].
8. Kushner RF, Schoeller DA. Estimation of total body water by bioelectrical impedance analysis. *Am J Clin Nutr*. 1986;44: 417—424.
9. Lukaski HC, Bolonchuk WW. Estimation of body fluid volumes using tetrapolar bioelectrical impedance measurements. *Aviat Space Environ Med*. 1988;59:1163—1169.
10. Segal KR, Van Loan M, Fitzgerald PI, Hodgdon JA, Van Itallie TB. Lean body mass estimation by bioelectrical impedance analysis: a four-site cross-validation study. *Am J Clin Nutr*. 1988;47:7—14.
11. Van Loan M, Mayclin P. Bioelectrical impedance analysis: is it a reliable estimator of lean body mass and total body water. *Hum Biol*. 1987;59:299—309.
12. Baumgartner RN, Chumlea WC, Roche AF. Bioelectric impedance for body composition. *Exerc Sport Sci Rev*. 1990;18:193—224.
13. Muraoka Y, Komiya S. Equation for estimating total body water by bioelectrical impedance measurements in Japanese subjects. *Ann Physiol Anthropol*. 1991;10:203—210 [in Japanese].
14. Lukaski HC, Bolonchuk WW, Hall CB, Siders WA. Validation of tetrapolar bioelectrical impedance method to assess human body composition. *J Appl Physiol*. 1986;60:1327—1332.
15. Merritt CR, Nagle HT, Grant E. Fabric-based active electrode design and fabrication for health monitoring clothing. *IEEE Trans Inf Technol Biomed*. 2009;13:274—280.
16. Gomez T, Mole PA, Collins A. Dilution of body fluid electrolytes affects bioelectrical impedance measurements. *Sports Med Training Rehab*. 1993;4:291—298.
17. Deurenberg P, Weststrate JA, Paymans I, van der Kooy K. Factors affecting bioelectrical impedance measurements in humans. *Eur J Clin Nutr*. 1988;42:1017—1022.
18. Brown BH, Karatzas T, Nakielny R, Clarke RG. Determination of upper arm muscle and fat areas using electrical impedance measurements. *Clin Phys Physiol Meas*. 1988;9:47—55.
19. Heymsfield SB, Gallagher D, Grammes J, Nuñez C, Wang Z, Pietrobelli A. Upper extremity skeletal muscle mass: potential of measurement with single frequency bioimpedance analysis. *Appl Radiat Isot*. 1998;49:473—474.
20. Pietrobelli A, Morini P, Battistini N, Chiumello G, Nuñez C, Heymsfield SB. Appendicular skeletal muscle mass: prediction from multiple frequency segmental bioimpedance analysis. *Eur J Clin Nutr*. 1998;52:507—511.
21. Fuller NJ, Hardingham CR, Graves M, Screaton N, Dixon AK, Ward LC, et al. Assessment of limb muscle and adipose tissue by dual-energy X-ray absorptiometry using magnetic resonance imaging for comparison. *Int J Obes Relat Metab Disord*. 1999; 23:1295—1302.
22. Lukaski HC. Assessing regional muscle mass with segmental measurements of bioelectrical impedance in obese women during weight loss. *Ann N Y Acad Sci*. 2000;904:154—158.
23. Elia M, Fuller NJ, Hardingham CR, Graves M, Screaton N, Dixon AK, et al. Modeling leg sections by bioelectrical impedance analysis, dual-energy X-ray absorptiometry, and anthropometry: assessing segmental muscle volume using magnetic resonance imaging as a reference. *Ann N Y Acad Sci*. 2000;904:298—305.
24. Cairns SP, Lindinger MI. Do multiple ionic interactions contribute to skeletal muscle fatigue? *J Physiol*. 2008;586: 4039—4054.
25. Cairns SP, Hing WA, Slack JR, Mills RG, Loiselle DS. Role of extracellular [Ca^{2+}] in fatigue of isolated mammalian skeletal muscle. *J Appl Physiol*. 1998;84:1395—1406.
26. Quiñonez M, González F, Morgado-Valle C, DiFranco M. Effects of membrane depolarization and changes in extracellular [K(+)] on the Ca (2+) transients of fast skeletal muscle fibers. Implications for muscle fatigue. *J Muscle Res Cell Motil*. 2010; 31:13—33.
27. Bouclin R, Charbonneau E, Renaud JM. Na^+ and K^+ effect on contractility of frog sartorius muscle: implication for the mechanism of fatigue. *Am J Physiol*. 1995;268:1528—1536.
28. Overgaard K, Nielsen OB, Clausen T. Effects of reduced electrochemical Na^+ gradient on contractility in skeletal muscle: role of the Na^+—K^+ pump. *Pflugers Arch*. 1997;434:457—465.
29. Nielsen OB, de Paoli F, Overgaard K. Protective effects of lactic acid on force production in rat skeletal muscle. *J Physiol*. 2001;536:161—166.
30. Pedersen TH, Nielsen OB, Lamb GD, Stephenson DG. Intracellular acidosis enhances the excitability of working muscle. *Science*. 2004;305:1144—1147.
31. Kristensen M, Albertsen J, Rentsch M, Juel C. Lactate and force production in skeletal muscle. *J Physiol*. 2005;562:521—526.
32. Usher-Smith JA, Xu W, Fraser JA, Huang CL. Alterations in calcium homeostasis reduce membrane excitability in amphibian skeletal muscle. *Pflugers Arch*. 2006;453:211—221.